Interactions of Water-Insoluble Tetraphenylporphyrins with Micelles Probed by UV−Visible and NMR Spectroscopy†,‡

ARTICLE *in* LANGMUIR · DECEMBER 1999

Impact Factor: 4.46 · DOI: 10.1021/la990903+

Interactions of Water-Insoluble Tetraphenylporphyrins with Micelles Probed by UV−Visible and NMR Spectroscopy†,‡

Martina Vermathen, Elizabeth A. Louie, Adam B. Chodosh, Sandra Ried, and Ursula Simonis*

Department of Chemistry & Biochemistry, San Francisco State University, San Francisco, California 94132

Received July 9, 1999. In Final Form: November 2, 1999

For developing clinically useful porphyrin drugs, it is essential to characterize porphyrin−membrane interactions and to determine the factors that modulate such interactions. To this end, four uniquely *p*-phenyl-substituted tetraphenylporphyrins were synthesized. These water-insoluble, unsymmetrically substituted porphyrins were allowed to diffuse into aqueous micellar solutions formed by the surfactants tetradecyltrimethylammonium bromide (TTAB), sodium dodecyl sulfate (SDS), and poly(ethylene glycol)-*p*-*t*-octylphenol (TX-100). The abilities of the porphyrins to localize in these micelles were determined by UV−vis and NMR spectroscopy. The data show that the NO_2−phenyl-substituted porphyrin did not diffuse into any of the micellar solutions. The COO^--substituted porphyrin was solubilized in cationic TTAB and in nonionic TX-100 micellar solutions under neutral and basic conditions. The NH_3^+-substituted porphyrin incorporated in anionic SDS micelles at pH = 2 and in TX-100 micelles at pH 2 and 7. These results emphasize that charge and polarity of the porphyrin substituent and its electrostatic interactions with the micelles play important roles in incorporating porphyrins with charged substituents into micelles. The OH−phenyl-substituted porphyrin incorporated into both neutral and basic TTAB and TX-100 micellar solutions in the highest concentrations, which reveals that a hydroxy substituent placed at the porphyrin periphery significantly increases the tendency of the porphyrin to embed in cationic and nonionic micelles. The data further demonstrate that all porphyrins are monodispersed in given micelles. In terms of porphyrin location, the data suggest that the COO^-− and NH_3^+−phenyl-substituted porphyrins localize in the hydrophobic interior of ionic micelles, whereas the OH−phenyl-substituted porphyrin adopts a location in the more polar domains of cationic micelles. In nonionic micelles, the COO^-−, NH_3^+−, and OH−phenyl-substituted porphyrins seem to orient themselves toward the water−micelle interface. An intercalation among the surfactant chains is proposed.

Introduction

Porphyrins and porphyrinoids are known to localize in tumor tissue and are, therefore, investigated with great interest in the medical and pharmaceutical industries.[1−16] Despite their potential applications in medicine and pharmacy, little is known about the reasons for the high affinity of tetrapyrrolic pigments to accumulate in tumor tissue, their uptake and delivery mechanisms into the cell, their localization patterns within the cell, and their cellular target(s).[2,10,17,18] In terms of cellular target(s), there is compelling evidence that both the plasma membrane[2,19] and subcellular membranous organelles, such as mitochondria,[2,4,10,18,20−25] are sensitive targets for the porphyrin

* To whom correspondence may be addressed at the Department of Chemistry & Biochemistry, San Francisco State University, 1600 Holloway Ave., San Francisco, CA 94132. Tel (415) 338-1656. FAX (415) 338-2384. E-mail: uschi@.sfsu.edu.

† Part of the Special Issue "Clifford A. Bunton: From Reaction Mechanisms to Association Colloids; Crucial Contributions to Physical Organic Chemistry.

‡ Presented in part as an invited talk at the 216th National Meeting of the American Chemical Society, Boston, MA, August 1998.

(1) Sternberg, E. D.; Dolphin, D. *Tetrahedron* **1998**, *54*, 4151−4202.
(2) Boyle, R.; Dolphin, D. *Photochem. Photobiol.* **1996**, *64* (3), 468−485.
(3) Dolphin, D. *Can. J. Chem.* **1994**, *72*, 1105−1110.
(4) Wöhrle, D.; Hirth, A.; Bogdahn-Rai, T.; Schnurpfeil, G.; Shopova, M. *Russ. Chem. Bull.* **1998**, *47*, 807−816.
(5) Fritsch, C.; Goerz, G.; Ruzicka, T. *Arch. Dermatol.* **1998**, *134*, 207−214.
(6) Ochsner, M. *J. Photochem. Photobiol.* **1997**, *39*, 1−19.
(7) Bissonnette, R.; Luis, H. *Lasers Dermatol.* **1997**, *15* (3), 507−519.
(8) Phillips, D. *Prog. React. Kinet.* **1997**, *22*, 175−300.
(9) Garbo, G. M. G. *J. Photochem. Photobiol.* **1996**, *34*, 1−19.
(10) Cannon, J. B. *J. Pharm. Sci.* **1993**, *82* (5), 435−446.
(11) Ni, Y.; Marchal, G.; Yu, J.; Lukito, G.; Petré, C.; Wevers, M.; Baert, A. L.; Ebert, W.; Hilger, C. S.; Maier, F. K.; Semmler, W. *Acad. Radiol.* **1995**, *2*, 687−699.
(12) Place, D. A.; Faustino, P. J.; van Zijl, P. C. M.; Chesnick, A.; Cohen, J. S. *Invest. Radiol.* **1990**, *25*, S69−S70.
(13) Bradshaw, J. E.; Gillogly, K. A.; Wilson, L. J.; Kumar, K.; Wan, X. M.; Tweedle, M. F.; Hernandez, G.; Bryant, R. G. *Inorg. Chim. Acta* **1998**, *276* (1-2), 106−116.
(14) Chen, W.; Mehta, S. C.; Lu, D. R. *Adv. Drug Delivery Rev.* **1997**, *26* (2-3), 231−247.
(15) Barth, R. F.; Soloway, A. H.; Brugger, R. M. *Cancer Invest.* **1996**, *14* (6), 534−550.
(16) Mehta, S. C.; Lu, D. R. *Pharm. Res.* **1996**, *13* (3), 344−351.
(17) (a) Kessel, D. *Photochem. Photobiol.* **1997**, *65* (3), 387−388. (b) Woodburn, K. W.; Fan, Q.; Miles, D. R.; Kessel, D.; Luo, Y.; Yound, S. W. *Photochem. Photobiol.* **1997**, *65* (3), 410−415.
(18) Berlin, K.; Jain, R. K.; Richerts, C. *Biotech. Bioeng. Comb. Chem.* **1998**, *61*, 106−118.
(19) Berg, K.; Moan, J. *Photochem. Photobiol.* **1997**, *65* (3), 403−409.
(20) Canete, M.; Villanueva, A.; Dominguez, V.; Polo, S.; Juarranz, A.; Stockert, J. C. *Int. J. Oncol.* **1998**, *13* (3), 497−504.
(21) Chatterjee, S. R.; Murugesan, S.; Kamat, J. P.; Shetty, S. J.; Srivastava, T. S.; Noronha, O. P. D.; Samuel, A. M.; Devasagayam, T. P. A. *Arch. Biochem. Biophys.* **1997**, *339* (1), 242−249.
(22) Chatterjee, S. R.; Srivastava, T. S.; Kamat, J. P.; Devasagayam, T. P. A. *Mol. Cell. Biochem.* **1997**, *166* (1-2), 25−33.
(23) (a) Richert, C.; Wessels, J. M.; Müller, M.; Kisters, M.; Benninghaus, T.; Goetz, A. E. *J. Med. Chem.* **1994**, *37*, 2797−2807. (b) Klein, S. D.; Walt, H.; Richter, C. *Arch. Biochem. Biophys.* **1997**, *348* (2), 313−319.
(24) Ricchelli, F.; Jori, G.; Gobbo, S.; Tronchin, M. *Biochim. Biophys. Acta* **1991**, *1065*, 42−48.
(25) (a) Ricchelli, F. *J. Photochem. Photobiol., B* **1995**, *29*, 109−118. (b) Ricchelli, F.; Gobbo, S.; Jori, G.; Salet, C.; Moreno, G. *Eur. J. Biochem.* **1995**, *233*, 165−170.

10.1021/la990903+ CCC: $19.00
Published on Web 12/11/1999

or porphyrinoid. There is also increasing evidence that the solubility of the pigment, i.e., its uptake and retention in membranes, is critical, if not a prerequisite for drug activity and efficacy.[18,27] Although pigment membrane solubility seems to correlate with both porphyrin/porphyrinoid and membrane characteristics,[1−12,24−27] structure−solubility and structure−activity relationships remain topics of great controversy.[1−4]

To characterize structure−solubility and −activity relationships, systematic studies of porphyrinic pigment membrane systems have to be carried out to determine (i) how membrane incorporation depends on structural, molecular, and electronic characteristics of the porphyrin/oid, (ii) how tetrapyrrolic pigments interact with membranes, and (iii) where in the membrane or at the membrane−water interface the tetrapyrrolic pigments are located. To this end, research groups, including our laboratory, have turned to the investigations of model membrane systems and have incorporated porphyrins into micelles and lipid bilayers.[18,24−44] These studies reveal that porphyrins can be solubilized and monodispersed in micelles.[31,32,36−41] However, it remains debated where at the micellar interface the porphyrin is located, if and how it is oriented, and how location and orientation correlate with structural characteristics of the pigment.[2,10,24−44] This is exemplified by reports, which show that the porphyrin macrocycle preferentially localizes inside the hydrophobic core of the micelle,[38] even in the presence of polar or charged peripheral substituents.[37−42] Protoporphyrin IX, for example, is described to reside in the hydrophobic region of a bilayer model membrane despite the two polar propionate chains.[24−26] Hematoporphyrin on the other hand, which is substituted by two additional alcohol groups, adopts a different orientation and interacts with the polar micelle headgroups.[26] Instead of being embedded in the hydrophobic interior of a model membrane, porphyrins with charged substituents are also described to bind peripherally to surfactant surfaces of opposite charges.[34,43] This, however, does not agree with findings demonstrating that porphyrins intercalate among the micelle-forming surfactant chains[40] with their polar substituents being placed close to the headgroup regions.[29,43,44] To add to the debate, it is also proposed that the location and orientation of porphyrins in model membranes can be tuned, such that charged porphyrins bind preferentially to the model membrane surface, whereas uncharged ones localize in the hydrophobic center.[34,35]

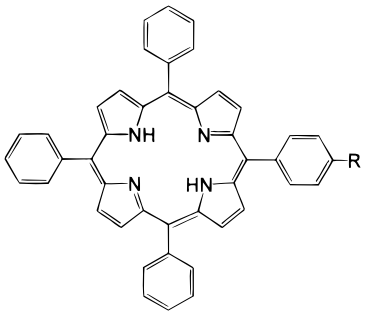

(**1**) R = NO_2 (p-NO_2)$_1$TPPH_2
(**2**) R = COOH (pH = 2) (p-COOH)$_1$TPPH_2
R = COO^- (pH > 6) (p-COO^-)$_1$TPPH_2
(**3**) R = OH (p-OH)$_1$TPPH_2
(**4**) R = NH_2 (neutral) (p-NH_2)$_1$TPPH_2
R = NH_3^+ (pH = 2) (p-NH_3^+)$_1$TPPH_2

Figure 1. Schematic representation of the structures of the mono *p*-phenyl-substituted tetraphenylporphyrins **1**−**4**.

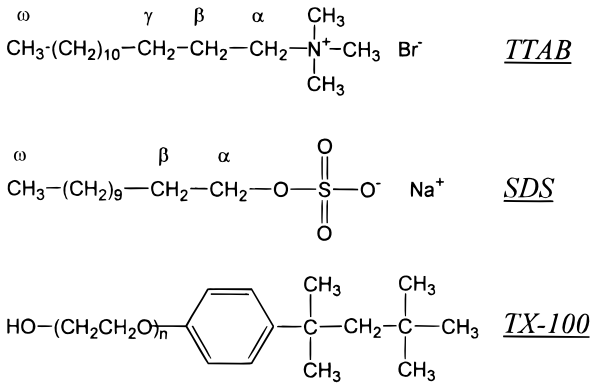

Figure 2. Schematic representation of the surfactants structures of tetradecyltrimethylammonium bromide (TTAB), sodium dodecyl sulfate (SDS), and poly(ethylene glycol)-*p*-*t*-octylphenol (TX-100) together with the labeling of the surfactant groups.

To test these hypotheses and to determine which factors modulate porphyrin−micelle interactions, four water-insoluble tetraphenylporphyrin (TPPH_2) derivatives (Figure 1) were synthesized and incorporated into aqueous solutions of cationic, anionic, and nonionic micelles (Figure 2). In this paper we will describe the methodology used for incorporating porphyrins (**1**−**4**) into micelles formed by the surfactants tetradecyltrimethylammonium bromide (TTAB), sodium dodecyl sulfate (SDS), and poly(ethylene glycol)-*p*-*t*-octylphenol (Triton X-100, TX-100) (Figure 2). We will also discuss the incorporation characteristics and the abilities of the porphyrins to localize in the micelles and show (i) that although water-insoluble, porphyrins (**2**−**4**) diffused freely into micelles, whereas (**1**) did not, (ii) that the ability of the pigments to localize in micelles depends on the nature of the porphyrin substituent, the surfactant headgroup, and the pH of the solution, (iii) that a hydroxy substituent placed at the periphery of the macrocycle significantly increases the tendency of the porphyrin to incorporate into micelles, and (iv) that both

(26) Ricchelli, F.; Gobbo, S. *J. Photochem. Photobiol., B* **1995**, *29*, 65−70.
(27) Hoebeke, M. *J. Photochem. Photobiol.* **1995**, *28*, 189−196.
(28) Schell, C.; Hombrecher, H. K. *Chem. Eur. J.* **1999**, *5* (2), 587−598.
(29) Brault, D.; Vever-Bizet, C.; Kuzelova, K. *J. Photochem. Photobiol., B* **1993**, *20*, 191−195.
(30) Vever-Bizet, C.; Brault, D. *Biochim. Biophys. Acta* **1993**, *1153* (2), 170−174.
(31) Kadish, K. M.; Maiya, B. G.; Araullo, C.; Guilard, R. *Inorg. Chem.* **1989**, *28*, 2725−2731.
(32) Kadish, K. M.; Maiya, B. G.; Araullo-McAdams, C. *J. Phys. Chem.* **1991**, *95*, 427−431.
(33) Maiti, N. C.; Mazumdar, S.; Periasamy, N. *J. Phys. Chem. B* **1998**, *102*, 1528−1538.
(34) Schenning, A. P. H. J.; Hubert, D. H. W.; Feiters, M. C.; Nolte, R. J. M. *Langmuir* **1996**, *12*, 1572−1577.
(35) Van Esch, J. H.; Feiters, M. C.; Peters, A. M.; Nolte, R. J. M. *J. Phys. Chem.* **1994**, *98*, 5541−5551.
(36) Minch, M. J.; La Mar, G. R. *J. Phys. Chem.* **1982**, *86*, 1400−1406.
(37) (a) Medhi, O. K.; Mazumdar, S.; Mitra, S. *Inorg. Chem.* **1989**, *28*, 3243−3248. (b) Mazumdar, S.; Medhi, O. K.; Mitra, S. *J. Chem. Soc., Dalton Trans.* **1990**, 1057−1061.
(38) Mazumdar, S. *J. Chem. Soc., Dalton Trans.* **1991**, 2091−2096.
(39) Mazumdar, S. *J. Phys. Chem.* **1990**, *94*, 5947−5953.
(40) Simplicio, J.; Schwenzer, K.; Maenpa, F. *J. Am. Chem. Soc.* **1975**, *97* (25), 7319−7326.
(41) Mazumdar, S.; Medhi, O. K.; Mitra, S. *Inorg. Chem.* **1988**, *27*, 7 (14), 2541−2543.
(42) Yushmanov, V. E. *Inorg. Chem.* **1999**, *38*, 1713−1718.
(43) Fuhrhop, J.-H.; Mathieu, J. *Angew. Chem., Int. Ed. Engl.* **1984**, *23*, 100−113.
(44) Cannon, J. B.; Kuo, F. S.; Pasternack, R. F.; Wong, N. M.; Müller-Eberhard, U. *Biochemistry* **1984**, *23*, 3715−3721.

Table 1. UV−Visible Absorption Band Maxima (λ_{max}) and Molar Absorption Coefficients (ϵ) of Porphyrins 1−4 in $CHCl_3$ and in 20 mM Aqueous Surfactant Solutions at 298 K

	λ_{max} [nm], (ϵ [10^3 M^{-1} cm^{-1}])				
porphyrin[a]	Soret B(0,0)	IV Q_y(1,0)	III Q_y(0,0)	II Q_x(1,0)	I Q_x(0,0)
(p-NO_2)$_1$TPPH$_2$ (**1**)					
$CHCl_3$	420	516 (15.3)	552 (7.2)	590 (4.7)	646 (3.1)
(p-COOH/COO^-)$_1$TPPH$_2$ (**2**)					
$CHCl_3$	420	516 (20)	552 (10)	592 (6.6)	646 (4.5)
TTAB (neutral)	419	516	552	592	648
TTAB (pH 10)	420	516	548	592	648
TX-100 (neutral)	420	514	548	592	648
TX-100 (pH 10)	420	514	548	592	646
(p-OH)$_1$TPPH$_2$ (**3**)					
$CHCl_3$	420	516 (16.5)	552 (7.6)	592 (5.1)	646 (3.6)
TTAB (neutral)	420	518	552	592	650
TTAB (pH 10)	420	514	550	592	648
TX-100 (neutral)	420	516	552	592	648
TX-100 (pH 10)	420	516	552	592	648
(p-NH_2/NH_3^+)$_1$TPPH$_2$ (**4**)					
$CHCl_3$	422	516 (13.3)	554 (7.3)	592 (4.5)	648 (3.9)
TX-100 (neutral)	420	516	552	592	648
TX-100 (pH 2)	420	514	550	592	648
SDS (pH 2)	438, 468[b]			598	656

[a] [Porphyrin] = 0.01−0.2 mM. [b] Split Soret band.

^{1}H and ^{13}C NMR chemical shift changes provide powerful means for probing porphyrin−micellar interactions and the average location of the porphyrin within the micelle.

Experimental Section

Instrumentation. UV−visible (UV−vis) spectra were recorded at 298 K in a thermostated cell on a Hewlett-Packard 8452A diode array spectrophotometer, which has a wavelength resolution of ±2 nm.

Proton and carbon-13 NMR spectroscopy were performed at 298 K on a BRUKER Avance DRX 300-MHz wide-bore spectrometer operating at resonance frequencies of 299.9200 and 75.4149 MHz for ^{1}H and ^{13}C, respectively.

Materials. If not stated otherwise, all chemicals and solvents were purchased from Fisher Scientific and were used without further purification. Tetradecyltrimethylammonium bromide (TTAB) was bought from Aldrich Chemical Co., and sodium dodecyl sulfate (SDS) and poly(ethylene glycol)-*p*-*t*-octylphenol (Triton X-100, TX-100) were purchased from Sigma. The deuterated NMR solvents obtained from Cambridge Isotopes were 99.9% enriched. The NMR spectra of the free base porphyrins were recorded in $CDCl_3$, whereas those of the micellar aggregates were acquired in D_2O. Abbreviations used are as follows: s = singlet, d = doublet, dd = doublet of doublets, m = multiplet. Column chromatography was done on silica gel, 60−200 mesh, whereas thin-layer chromatography (TLC) was performed on commercially prepared Machery-Nagel Polygram SIL G/UV slica gel TLC plates.

Syntheses of Porphyrins 1−3. The porphyrins *5*-(*p*-nitro)-phenyl-10,15,20-triphenylporphyrin (p-NO_2)$_1$TPPH$_2$ (**1**), *5*-(*p*-carboxy)phenyl-10,15,20-triphenylporphyrin (p-COO^-)$_1$TPPH$_2$ (**2**), which in acidic solution converts to (p-COOH)$_1$TPPH$_2$, and *5*-(*p*-hydroxy)phenyl-10,15,20-triphenylporphyrin (p-OH)$_1$TPPH$_2$ (**3**) are not commercially available and were synthesized by the mixed aldehyde approach.[45a] Three equivalents of benzaldehyde (0.15 mol, 15.92 g) and 1 equiv (0.05 mol) of *p*-nitrobenzaldehyde (7.56 g), *p*-carboxybenzaldehyde (7.51 g), or *p*-hydroxybenzaldehyde (6.11 g) were reacted with 4 equiv (0.2 mol) of pyrrole in propionic acid. The obtained porphyrinic mixtures contained in addition to the desired mono-*p*-phenyl-substituted TPPH$_2$ derivatives, unsubstituted, di-, tri-, and tetraphenyl-substituted porphyrins. The porphyrins were separated by column chromatography on silica gel. Porphyrins **1**, **2**, and **3** were eluted from the columns as second bands with mixtures of $CHCl_3$/cyclohexane (8:2), $CHCl_3$/CH_2Cl_2/ethyl acetate/methanol (45:50:3.5:1.5), and toluene, respectively. The UV−vis absorption maxima of the porphyrin Q and the Soret bands in $CHCl_3$ and their molar absorption coefficients in 10^3 M^{-1} cm^{-1} are listed in Table 1.

^{1}H NMR data of 1: δ (ppm) −2.779 (s, 2 H, α-pyrrole NH), 7.731−7.802 (m, 9 H, phenyl-$H_{m,p}$), 8.218 (dd, 6 H, phenyl-H_o, J = 7.31 Hz), 8.401 (d, 2 H, NO_2-phenyl-H_m, J = 8.78 Hz), 8.641 (d, 2 H, NO_2-phenyl-H_o, J = 8.78 Hz), 8.743 (d, 2 H, β-pyrrole H, J = 4.76 Hz), 8.867 (s, 4 H, β-pyrrole H), 8.898 (d, 2 H, β-pyrrole H, J = 4.75 Hz).

^{1}H NMR Data of 2: δ (ppm) −2.772 (s, 2 H, α-pyrrole NH), 7.729−7.797 (m, 9 H, phenyl-$H_{m,p}$), 8.223 (dd, 6 H, phenyl-H_o, J = 7.31 Hz), 8.360 (d, 2 H, COOH-phenyl-H_m, J = 8.05 Hz), 8.516 (d, 2 H, COOH-phenyl-H_o, J = 8.05 Hz), 8.807 (d, 2 H, β-pyrrole H, J = 4.39 Hz), 8.857 (s, 4 H, β-pyrrole H), 8.882 (d, 2 H, β-pyrrole H, J = 5.13 Hz).

^{1}H NMR Data of 3: δ (ppm) −2.777 (s, 2 H, α-pyrrole NH), 7.214 (d, 2 H, OH-phenyl-H_m, J = 8.79 Hz), 7.728−7.790 (m, 9 H, phenyl-$H_{m,p}$), 8.080 (d, 2 H, OH-phenyl-H_o, J = 8.78 Hz), 8.216 (dd, 6 H, phenyl-H_o, J = 7.32 Hz), 8.838 (s, 4 H, β-pyrrole H), 8.844 (d, 2 H, β-pyrrole H, J = 3.66 Hz), 8.879 (d, 2 H, β-pyrrole H, J = 5.12 Hz).

Synthesis of Porphyrin 4. 5-(*p*-Aminophenyl)-10,15,20-triphenylporphyrin (p-NH_2)$_1$TPPH$_2$ **(4)**, which converts to (p-NH_3^+)$_1$TPPH$_2$ in acidic solution, was prepared from (p-NO_2)$_1$-TPPH$_2$ (**1**) by dissolving 7.58×10^{-5} mol (=0.050 g) of **1** in glacial acetic acid and reducing it with 6.6×10^{-4} mol (=0.150 g) of $SnCl_2 \cdot 2H_2O$ (Aldrich Chemical Co.) in 10 mL of 12 M HCl as described by Collman et al.[46] The desired porphyrin **4** was purified by column chromatography on silica gel and eluted with CH_2Cl_2. The UV−vis data of **4** are summarized in Table 1.

^{1}H NMR data of 4: δ(ppm) −2.754 (s, 2 H, α-pyrrole NH), 4.034 (s, 2 H, phenyl-NH_2), 7.072 (d, 2 H, NH_2-phenyl-H_m, J = 8.41 Hz), 7.715−7.788 (m, 9 H, phenyl-$H_{m,p}$) 8.000 (d, 2 H, NH_2-phenyl-H_o, J = 8.42 Hz), 8.217 (d, 6 H, phenyl-H_o, J = 7.68 Hz), 8.827−8.842 (m, 6 H, β-pyrrole H), 8.943 (d, 2 H, β-pyrrole H, J = 4.75 Hz).

Porphyrin Characterizations. All porphyrins were characterized unambiguously by UV−vis and ^{1}H NMR spectroscopy and by comparing the extinction coefficients and the ^{1}H chemical shifts and resonance patterns to those available in the literature.[45,46] The purities of the porphyrins were determined by TLC, high-performance liquid chromatography (HPLC), UV−vis, and ^{1}H NMR spectroscopy.

(45) (a) Adler, A. D.; Longo, F. R.; Finarelli, J. D.; Goldmacher, J.; Assour, J.; Koraskoff, L. *J. Org. Chem.* **1967**, *32*, 476. (b) Kong, J. L. Y.; Loach, P. A. *Heterocycl. Chem.* **1980,** *17*, 737. (c) Gunduz, N.; Gunduz, T.; Hayvali, M. *Talanta* **1999,** *48* (1), 71.

(46) Collman, J. P.; Brauman, J. I.; Doxsee, K. M.; Halbert, T. R.; Bunnenberg, E.; Linder, R. E.; LaMar, G. N.; Del Gaudio, J.; Lang, G.; Spartalian, K. *J. Am. Chem. Soc.* **1980**, *102* (12), 4182−4192.

Table 2. Porphyrin Concentrations (mM) in the Micellar Solutions As Determined by UV−Visible Spectroscopy at 298 K

	TTAB			SDS			TX-100		
	1/100[d]	1/50[d]	1/20[d]	1/100[d]	1/50[d]	1/20[d]	1/100[d]	1/50[d]	1/20[d]
$(p\text{-}NO_2)_1TPPH_2$[a]	*b*	*b*	*b*	*b*	*b*	*b*	*b*	*b*	*b*
$(p\text{-}NH_2)_1TPPH_2$, neutral	*b*	*b*	*b*	*b*	*b*	*b*	0.16	0.29	0.35
$(p\text{-}NH_3^+)_1TPPH_2$, pH 2	*b*	*b*	*b*	0.15	0.17	0.21	0.14	0.22	0.57
$(p\text{-}COO^-)_1TPPH_2$, neutral	0.21	0.22	0.22	*b*	*b*	*b*	0.13	0.18	0.22
$(p\text{-}COO^-)_1TPPH_2$, pH 10	0.15	0.23	0.30	*c*	*c*	*c*	0.14	0.24	0.29
$(p\text{-}OH)_1TPPH_2$, neutral	0.17	0.23	0.71	*b*	*b*	*b*	0.20	0.17	1.36
$(p\text{-}OH)_1TPPH_2$, pH 10	0.10	0.14	0.16	*c*	*c*	*c*	0.03	0.21	1.09

[a] Porphyrin insoluble at pH 2, 7, and 10, and at 298 and 323 K. [b] Porphyrin concentration in micellar solution <0.05 mM. [c] Not determined (SDS precipitates at pH 10). [d] Porphyrin/surfactant ratio.

Incorporation of Porphyrins 1−4 into TTAB, SDS, and TX-100 Micellar Solutions. Each of the porphyrin micelle solutions was prepared from 20 mM TTAB, SDS, or TX-100 surfactant stock solutions by dissolving calculated amounts of either TTAB (67.28 mg), SDS (57.68 mg), or TX-100 (100 mg) in 10 mL of D_2O or in 10 mL of a D_2O-based buffer solution (ND_4Br/ND_4OD, pH = 10; ND_4Br/DBr, pH = 2). To ensure that micelles were formed, the work was carried out at surfactant concentrations (20 mM) well above the critical micelle concentrations (cmc's) for each of the surfactants.[47−49] Calculated aliquots of a 1.0 mM (1 mL) or a 0.2 mM (1 or 2 mL) porphyrin solution in chloroform (Fisher, HPLC grade) were transferred into 8 mL glass vials. The solvent was evaporated under a stream of purified argon to leave a thin layer of finely dispersed porphyrin on the bottom of each of the vials. To prepare solutions with porphyrin/surfactant molar ratios of 1/100, 1/50, and 1/20, a calculated amount of each of the 20 mM surfactant stock solutions (1 mL) was carefully added to the vials containing the dried porphyrin layers. The porphyrin micellar solutions were left standing and allowed to equilibrate at room temperature for an additional 5 days. After the 5-day equilibration period, undissolved porphyrin remained in most of the solutions. Therefore, the concentrations of each of the porphyrins in a given micellar solution were determined by UV−vis spectroscopy. To ensure that 5 days provided enough time for the equilibration and diffusion process, longer periods were also used. Even after 20 days, the porphyrin concentrations in the micellar solution remained unchanged demonstrating that each of the porphyrins has a specific affinity for a given micellar solution. However, in TX-100 micellar solutions the entire porphyrin amounts dissolved completely after approximately 3 months.

UV−Visible Spectroscopy Measurements. The UV−vis spectra of both the free base porphyrins and the porphyrin micellar aggregates were measured at 298 K using 1.0-cm quartz cuvettes. To determine the molar extinction coefficients of the porphyrin Soret bands, the solutions were either diluted or 0.9-cm quartz spacers were used. The UV−vis data of the free base porphyrins and those of the porphyrins incorporated in the micelles are summarized in Table 1. Since the porphyrins did not dissolve completely in most of the surfactant solutions, the actual porphyrin concentrations in the aqueous micellar surfactant solutions were determined spectrophotometrically and were calculated according to Lambert−Beer's law[26,34] from the absorption maxima of the Q-bands I−IV using a calibration for each porphyrin in chloroform. All absorbances were measured in the linear regime of Lambert−Beer's law. For the calibration, the UV−vis absorption spectra of each of the porphyrins dissolved in chloroform at four known concentrations in the range of 0.01−0.2 mM were measured. Plots of porphyrin concentrations versus Q-band absorption (at λ_{max}) were analyzed by linear regression ($r^2 > 0.96$) to yield the calibration curve from which the porphyrin concentrations in the micellar aggregates were determined. These concentrations are summarized in Table 2. Values are not corrected for different molar absorptivities, since the porphyrins are water-insoluble.

NMR Spectroscopy. The ^1H NMR spectra were recorded at 298 K with the one-pulse sequence (zg) available in the BRUKER pulse sequence library using an inverse-detected multinuclear probe. Typically, 8−32 transients, a spectral width of 5708 Hz, a data size of 32K points, an acquisition time of 2.87 s, and a relaxation delay of 1.0 s were used to acquire the ^1H NMR spectra. The free induction decays (FIDs) were signal-averaged, apodized with a line broadening factor of 0.1 Hz, Fourier transformed, and phase corrected. Chemical shifts were referenced to DSS (2,2-dimethyl-2-silapentane-5-sulfonate) as internal standard ($\delta(Si(CH_3)_3) = 0.000$ ppm) for the D_2O solutions and to the residual proton resonance of $CDCl_3$ at 7.260 ppm for the chloroform solutions. The chemical shift values of resonances not experiencing appreciable line broadening are given with an accuracy of ±0.002 ppm. Proton-decoupled ^{13}C NMR spectra were recorded with a four-nuclei QNP probe using the one-pulse sequence zgdc (WALTZ-16 decoupling, BRUKER pulse sequence library). The ^{13}C NMR spectra were typically recorded with a data size of 32K, a spectral width of 9578 Hz, and a relaxation delay of 1.0 s to give an acquisition time of 1.71 s. At least 1280 transients were signal-averaged. The data were apodized with a line-broadening factor of 1.0 Hz prior to Fourier transformation. The ^{13}C NMR spectra were referenced to DSS as external standard ($\delta(Si(CH_3)_3) = 0.000$ ppm). Spin−lattice relaxation times, T_1, of the surfactant protons were measured using the inversion recovery sequence t1ir (BRUKER pulse sequence library) with a variable delay time τ between the 180° and 90° pulses. The τ delays were varied from 0.05 to 6 s for TTAB, 0.1 to 10 s for SDS, and 0.01 to 5 s for TX-100 ($\approx 5T_1$). The T_1 relaxation times were calculated from an intensity fit of the data using the fitting program available in the BRUKER processing software.

Results and Discussion

Syntheses and Incorporation of Porphyrins 1−4 into Micelles. In our ongoing study to characterize porphyrin model−membrane interactions and to comprehend how molecular, structural, and electronic properties of the porphyrin and the characteristics of the micelle modulate such interactions and the ability of the porphyrin to incorporate into given micelles, four tetraphenylporphyrins (Figure 1) were synthesized and allowed to diffuse into cationic, anionic, and nonionic micelles at various pH. In this paper, porphyrins **1**−**4**, namely, 5-(*p*-nitro)-phenyl-10,15,20-triphenylporphyrin, $(p\text{-}NO_2)_1TPPH_2$ (**1**), 5-(*p*-carboxy)phenyl-10,15,20-triphenylporphyrin, $(p\text{-}COO^-)_1TPPH_2$ **2**, 5-(*p*-hydroxy)phenyl-10,15,20-triphenylporphyrin, $(p\text{-}OH)_1TPPH_2$ **3**, and 5-(*p*-amino)phenyl-10,15,20-triphenylporphyrin, $(p\text{-}NH_2)_1TPPH_2$ **4** are categorized according to their relative polarities. Porphyrins **2**−**4** are classified as "polar" pigments when compared to the less polar porphyrin **1**. All porphyrins are water-insoluble and differ only in charge and polarity of the unique substituent, which is placed in the para position of one of the phenyl rings (Figure 1). The nature of this substituent was expected to provide the porphyrins with an incentive to diffuse into micellar solutions of specific characteristics and to adopt preferred orientations. To ensure that conclusions drawn in regard to the factors that modulate

(47) (a) Rosen, M. J. *Surfactants and Interfacial Phenomena*; John Wiley & Sons: New York, 1978; p 96. (b) Evans, D. F.; Wennerström, H. *The Colloidal Domain*; Wiley−VCH: New York, 1999; p 190.
(48) Kratohvil, J. P. *J. Colloid Interface Sci.* **1980**, *75*, 271−275.
(49) Jones, M. N.; Chapman, D. *Micelles, Monolayers, and Biomembranes*; Wiley-Liss, Inc.: New York, 1995; p 68.

the ability of a porphyrin to embed in micellar solutions are not influenced by characteristics other than those of the porphyrin or the micelles, the experimental conditions were carefully monitored and an alternative method to the sonication procedure typically employed[24−43] was used for incorporating the porphyrins into the micellar solutions. The porphyrins in finely dispersed form were allowed to diffuse into cationic TTAB, anionic SDS, and nonionic TX-100 micellar solutions at concentrations well above the cmc's of each of these surfactants.[47−49] The surfactant cmc's that were determined by ^{1}H NMR spectroscopy from the first breakpoint of a graph, in which the ^{1}H chemical shifts are plotted as function of the inverse of increasing surfactant concentration,[50] agree well with values determined by other methods (TTAB, 3.8 mM at 298 K;[47] SDS, 8.1 mM at 298 K;[48] and TX-100, 0.24 mM at 298 K[49]). As will be discussed in more detail below, each of the porphyrins dissolved in micelles of specific characteristics with the exception of **1**, which did not diffuse into any of the micellar solutions. As the best compromise for all three micellar systems, the surfactant concentrations were kept constant at 20 mM, since the chemical shifts for each of the surfactants remained essentially unchanged in a concentration range of 15−50 mM for TTAB, 15−25 mM for SDS, and 5−25 mM for TX-100. Furthermore, at 20 mM surfactant concentration, the majority of micelles contained porphyrins at least at porphyrin/surfactant molar ratios of 1:20 assuming that the porphyrins are monodispersed in micelles. Such an assumption is supported by compelling evidence, which reveals that porphyrins are monodispersed in micelles at low pigment/surfactant ratios.[31,32,36−41] No attempts were made to incorporate porphyrins into micelles at ratios exceeding of 1:20 due to the likelihood of porphyrin aggregate formation. The porphyrin/surfactant ratios were selected to be greater or equal than 1/*N*, with *N* representing the average surfactant aggregation number. At these ratios, it can be estimated that one porphyrin molecule is solubilized by a single micelle, and therefore, it is assured that the changes observed in both the UV−vis and NMR spectra are caused by porphyrin micellar interactions.

UV−Visible Spectroscopy. UV−vis spectroscopy was used to determine which characteristics of the porphyrin and/or the micelle modulate the ability of the porphyrin to diffuse into a given micellar solution. As is typically observed,[31,32,52] the UV−vis spectra of porphyrins **1**−**4** either in the aqueous micellar TTAB, SDS, and TX-100 solutions or in chloroform give rise to the four porphyrin Q-bands (I−IV) in the spectral region of 514−650 nm and to a Soret band centered at 420 nm. The absorption band maxima in both solvent systems are summarized in Table 1. All porphyrin micellar concentrations in dependence of the initial molar porphyrin/surfactant ratios are listed in Table 2. These concentrations, which increase with increasing initial porphyrin/surfactant ratios to reach a maximum in solutions with ratios of 1:20, illustrate that each of the water-insoluble porphyrins has a limited solubility in a given micellar solution and that the ability of a porphyrin to diffuse into such solutions is modulated by the nature of the porphyrin substituent and the characteristics of the micelle. Porphyrin **1** did not diffuse into any of the micellar solutions under any of the experimental conditions employed. Porphyrins **2** and **4** incorporated into nonionic TX-100 micellar solutions, but only into ionic micelles when the surfactant headgroup charges were opposite to those of the porphyrin substituents. Porphyrin **3** dissolved in cationic TTAB and in nonionic TX-100 micellar solutions. Similar observations were made by Van Esch et al.[35] who showed that the amounts of porphyrin that incorporate into bilayers of dioctyldecyldimethylammonium (DODAC) increase with increasing porphyrin/surfactant molar ratios and that the abilities of the porphyrins to embed in micelles are modulated by the nature of the porphyrin substitutent.

Absorption Band Maxima. The UV−vis absorption band maxima of the porphyrin Q-bands (Table 1) were measured in both aqueous micellar and chloroform solutions to characterize the environments, in which porphyrins **2**−**4** reside upon their incorporation into the micellar interfaces. When compared to chloroform, the absorption maxima of the porphyrin Q-bands in the micellar solutions remain essentially unchanged and do not experience any red-shifts. This indicates that, when dissolved in micelles, porphyrins **2**−**4** localize in an environment that has a similar polarity to that of chloroform. Therefore, it can be assumed that the porphyrins incorporate in the hydrophobic interior of the micelles and that they are not simply adsorbed to the micellar surfaces surrounded by the aqueous bulk phase. This conclusion agrees well with reports, which show that the UV−vis absorption band maxima are red-shifted, when a water-insoluble porphyrin changes its environment from a hydrophobic to a hydrophilic one, or when a water-soluble porphyrin is incorporated from the aqueous bulk phase into the hydrophobic micellar core.[27,31,32,53−55] The data therefore support the notion that the transfer from a nonpolar to a polar solvent, such as chloroform to water, or vice versa, alters the electronic state of the solutes resulting in red-shifts of their absorption bands.

To establish that the porphyrins are monodispersed within given micelles, the porphyrin Soret bands centered at 420 nm were further examined. With the exception of the UV−vis spectra of **4**, (p-NH_3^+)$_1$TPPH$_2$, in SDS at pH = 2, the electronic spectra of all other porphyrins in the micellar solutions reveal a single, nonsplit Soret band (Table 1), which can be taken as evidence that the porphyrins are monodispersed within given micelles.[31,32,36−41] However, when **4** was incorporated into a SDS solution at pH 2, a split Soret band with absorption maxima at 438 and 468 nm was obtained in the UV−vis spectrum. Although the splitting of the Soret band serves commonly as indicator of porphyrin dimer or aggregate formation,[31,32] for (p-NH_3^+)$_1$TPPH$_2$ in acidic SDS micelles aggregation can be ruled out on the basis of the observation that the four-banded spectrum in neutral micellar solution collapses into a two-banded spectrum at pH = 2.[35,51,52] The split Soret band and the two-banded spectrum observed for (p-NH_3^+)$_1$TPPH$_2$ in acidic SDS micellar solution can, therefore, be ascribed to the protonation of all inner porphyrin nitrogen atoms,[52] which is consistent with the observation that the solution turns from red to green at low pH. Additional proof that porphyrin dimer or aggregate formation can be ruled out is given by the UV−vis data of **4** in neutral and acidic TX-100 solution.

(50) Vermathen, M.; Bachofer, S. J.; Simonis, U. Manuscript in preparation.

(51) (a) Kasha, R.; Rawls, H. R.; Asraf El-Bayoumoi, M. *Pure Appl. Chem.* **1965**, *11*, 371. (b) Hunter, C. A.; Sanders, J. M. K.; Stone, A. *Chem. Phys.* **1989**, *133*, 395−404.

(52) (a) Smith, K. M. In *Porphyrins and Metalloporphyrins*; Smith K. M.; Ed.; Elsevier Scientific Publishing Co.: Amsterdam, 1975; p 24. (b) Milgrom, L. R. Porphyrins of the Future. In *Colours of Life*; Milgrom, L. R., Ed.; Oxford University Press: Oxford, 1997; pp 84−89.

(53) Vermathen, M.; Simonis, U. Unpublished results.

(54) Brault, D.; Vever-Bizet, C.; Le Doan, T. *Biochim. Biophys. Acta* **1986**, *857*, 238−250.

(55) Brault, D.; Vever-Bizet, C.; Delinger, M. *Biochimie* **1986**, *68*, 913−921.

For these solutions, the characteristic four-banded visible spectrum with a single, nonsplit Soret band centered at 420 nm is observed. If **4** would tend to aggregate in acidic SDS solution, one would expect to observe this tendency also in TX-100 micelles. Quite surprisingly, the incorporation of **4** into TX-100 micelles at pH 2 did not result in the protonation of all inner nitrogen atoms. The solution remained red, which gives rise to speculations that TX-100 acts as a proton sponge.

The conclusion that all porphyrins, including **4**, are monodispersed in TTAB, SDS, and TX-100 micelles, even at porphyrin-to-surfactant ratios of 1:20, is also supported, when the surfactant aggregation numbers and the surfactant/porphyrin ratios are taken into account. It is well established that tetraphenylporphyrins are monodispersed in micelles, when the surfactant/porphyrin ratios are larger than the average aggregation number.[31,32] This is the case for all porphyrin micellar systems with the exception of the highest concentrated (0.710 mM) TTAB sample. All other SDS/(p-NH_3^+)$_1$TPPH_2, TTAB/(p-COOH/COO^-)$_1$TPPH_2, and TTAB/(p-OH)$_1$TPPH_2 micelles have surfactant/porphyrin ratios that are larger than the average aggregation number, assuming average aggregation numbers of 70, 58, and 140 for aqueous solutions of TTAB, SDS, and TX-100, respectively.[48] Considering the porphyrin/surfactant ratios and the actual porphyrin concentrations of each of the micellar solutions (Table 2), it can be estimated that each micelle formed incorporates one porphyrin molecule. However, it should be cautioned that the micelle/porphyrin ratios are only rough estimates, since it cannot be ruled out that the incorporation of porphyrins into micelles may alter their usual spherical geometry and may lead to a different reassembly of the surfactant molecules with altered aggregation numbers. We are currently in the process of determining the aggregation number of each of the porphyrin micellar systems to also characterize the size and shape of the porphyrin micellar aggregates.[56]

Porphyrin Abilities to Incorporate into Micellar Solutions. Since all four tetraphenylporphyrins investigated in this study are water-insoluble, the concentrations of porphyrins **2**−**4** in the micellar solutions reflect their relative ability to diffuse freely into micelles of given characteristics (Table 2). Among the porphyrins, large differences exist in their abilities to incorporate into micellar solutions. The maximum porphyrin concentrations in the micelles vary considerably from 0.1 to 1.3 mM depending on the pH of the solution and the nature of the porphyrin and the micellar aggregate. The TPPH_2 with the least polar p-phenyl substituent, (p-NO_2)$_1$TPPH_2, showed no tendency to incorporate into either cationic, anionic, or nonionic micellar solutions. Even at modified experimental conditions (change in pH from 2 to 10 and change in temperature from 298 to 323 K), this porphyrin remained insoluble in the micellar solutions, suggesting that it does not have the right balance between hydrophobicity and hydrophilicity to embed in ionic or nonionic micelles. In support of this notion, similar behaviors were observed for monosubstituted 5-(p-fluoro, -chloro, or -bromo)phenyl-10,15,20-triphenylporphyrins, which did also not diffuse into any of the micellar solutions.[53]

Abilities of Porphyrins 2−4 to Incorporate into TX-100 Micelles. Replacement of the NO_2 group with more polar or charge bearing OH-, COO^-/COOH-, or NH_2/NH_3^+-substituents increases the hydrophilicity of the porphyrins **2**−**4** and enables them to diffuse into nonionic TX-100 micellar solutions independent of the charge or polarity of the substituent. The greatest tendency to incorporate into TX-100 micelles was observed for (p-OH)$_1$TPPH_2 at pH = 7 and 10 with concentrations of 1.36 and 1.09 mM, respectively, followed by (p-NH_3^+)$_1$TPPH_2 in acidic solution (0.57 mM) (Table 2). The COO^--substituted porphyrin **2** in TX-100 showed the least tendency to diffuse into nonionic micelles (0.13−0.29 mM). These results allow us to conclude that TX-100 micelles solubilize porphyrins with at least one substituent that is more polar than a NO_2 group. In addition to charge and polarity of the porphyrin substituent, its capability to form hydrogen bonds to water at the water−micelle interface may have to be considered an important contributor to the solubilization of the porphyrins in nonionic micelles.

Ability of Porphyrin 4 to Incorporate into SDS Micelles. In anionic SDS micellar solutions, porphyrin **4** dissolved only under acidic conditions. The pigment remained undissolved in neutral SDS micelles. This finding can be explained when one considers that under acidic conditions the amine substituent is protonated and (p-NH_3^+)$_1$TPPH_2 is formed. It is therefore quite reasonable to assume that the positive charge of the NH_3^+ substituent enables the porphyrin to incorporate at low pH into anionic micelles, i.e., into micelles with oppositely charged headgroups, which agrees with the observation that (p-NH_3^+)$_1$-TPPH_2 did not incorporate into cationic TTAB micelles. Consequently, it can be concluded that porphyrins with positively charged substituents do not embed in micelles with positively charged headgroup and that substituent and headgroup charge and the electrostatic interactions between the porphyrin substituent and the headgroups play important roles in solubilizing porphyrin **4** in micelles. The alternative explanation, that the protonation of all pyrrole nitrogen atoms is the driving force for porphyrin **4** to dissolve in SDS micelles at pH 2 can be ruled out, since (p-NO_2)$_1$TPPH_2 does not diffuse into SDS micelles under acidic conditions despite the protonation of all four pyrrole nitrogen atoms. In fact, it is discussed that the protonation of all nitrogen atoms reduces the hydrophobicity of the porphyrin core thereby preventing porphyrin incorporation into a given micelle.[25] The affinity of (p-NH_3^+)$_1$TPPH_2 toward SDS micelles is therefore attributable to the cationic nature of the porphyrin substituent and the anionic nature of the headgroups. Other researchers have arrived at similar conclusions.[24−26,31,32] However, Schenning et al.[34] report that pyridinium-substituted tetraarylporphyrins incorporate into positively charged DODAC bilayers. This either suggests that bilayers solubilize porphyrins in a different way or that the methodology employed forced the porphyrin to embed into this bilayer.

Abilities of Porphyrins 2 and 3 to Incorporate into TTAB Micelles. In support of the notion that substituent charge plays an important role in dissolving porphyrins in micelles, it was observed that *(p-COO^-)$_1$TPPH_2* was soluble in neutral and basic TTAB but not in anionic SDS micellar solutions. The concentrations of (p-COO^-)$_1$TPPH_2 in TTAB and TX-100 in neutral solutions are low and of comparable magnitude with a maximum concentration of ≈0.2 mM for all three initial porphyrin/surfactant ratios of 1:100, 1:50, and 1:20 (Table 2). At pH 10, the porphyrin concentrations in TTAB and TX-100 solutions are also comparable. However, at this pH, the solubility of the porphyrin increases with increasing porphyrin concentrations to reach a maximum at initial porphyrin/surfactant ratios of 1:20. As observed for *(p-COO^-)$_1$TPPH_2*, and in agreement with reported data,[25a,54,55] porphyrin **3**, *(p-OH)$_1$TPPH_2*, dissolved also in neutral and basic TTAB

(56) Vermathen, M.; Louie, E. A.; Simonis, U. Manuscript in preparation.

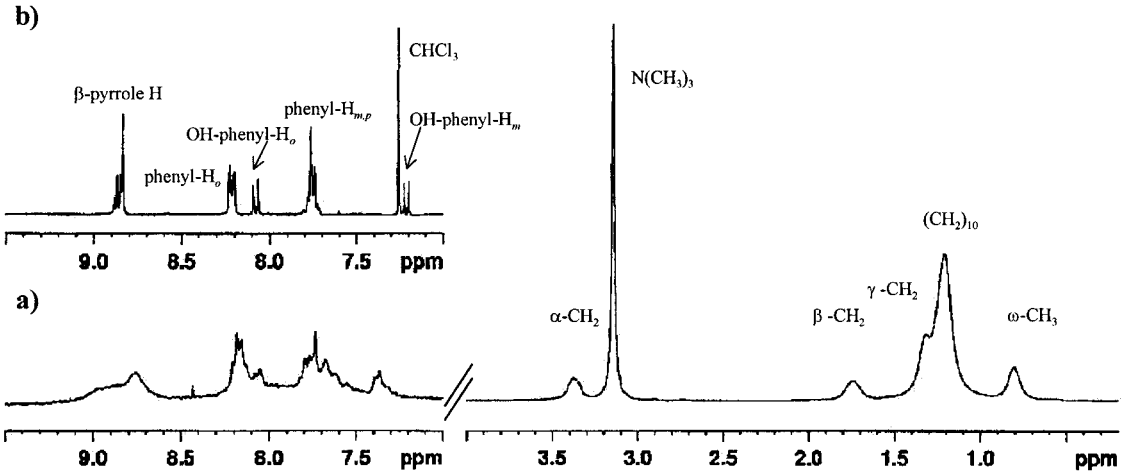

Figure 3. ^{1}H NMR spectrum of (p-OH)$_1$TPPH$_2$ (a) in 20 mM TTAB solution and (b) in $CDCl_3$. Note the resonance broadening and chemical shift changes when the porphyrin is incorporated into TTAB micelles.

micellar solutions. However, it incorporated to the greatest extent in neutral TX-100 solution (maximum porphyrin concentration 1.36 mM). This brings again to mind that hydrogen bond formation of the porphyrin substituent to water at the water/micelle interface may be of great importance for solubilizing *(p-OH)$_1$TPPH$_2$* in TTAB and TX-100 micelles, which agrees with the suggestion that *(p-OH)$_1$TPPH$_2$* localizes in the polar domains of these micelles, as is outlined in the NMR section below.

NMR Spectroscopy. NMR spectroscopy was used as vital tool to substantiate the conclusions drawn from the analysis of the UV−vis spectroscopic data and to obtain a better understanding of the factors that modulate porphyrin−micellar interactions. To determine whether porphyrins **2**−**4** localize preferentially in the hydrophobic regions of the micelle interior or at the water−micellar interface and to deduce the orientation and average location of these porphyrins within the micellar aggregates, the chemical shift trends observed for the surfactant resonances of all solutions with porphyrin concentrations above 0.05 mM were investigated by ^{1}H and, for selected systems, also by ^{13}C NMR spectroscopy. For reasons outlined below, the resonances of the tetraphenylporphyrins were of low diagnostic value. To ascertain that the observed chemical shift changes of the surfactant resonances arise from porphyrin−micellar interactions and not from changes in surfactant concentrations, all surfactant concentrations were kept constant at 20 mM, and solely the porphyrin concentrations were varied. For a selected system, namely for (p-COO$^-$)$_1$TPPH$_2$/TTAB, the experiments were repeated in 50 mM TTAB solution.[57] Similar chemical shift changes were observed for the surfactant resonances of the 50 and 20 mM porphyrin micellar solutions confirming that the observed chemical shift trends are caused by the anisotropy effect of the porphyrin macrocycle. The surfactant resonance assignments of TTAB, SDS, and TX-100 agree with those reported in the literature[31,32,58,59] and are, therefore, not further discussed. Figure 3 gives a representative ^{1}H NMR spectrum of (p-OH)$_1$TPPH$_2$ in TTAB micelles at 298 K with the surfactant protons resonating in the spectral region of 0.6−3.4 ppm and those of the porphyrin and phenyl rings giving rise to the signals at 7.0−9.3 ppm. For comparative reasons, the spectrum of the free base porphyrin recorded in $CDCl_3$ is shown in Figure 3b together with the resonance assignments. Note that the spectral region of the phenyl and porphyrin ring resonances in Figure 3a is not drawn to scale. The region is blown up by a factor of 5 to depict all resonances.

As is exemplified in Figure 3a for the (p-OH)$_1$TPPH$_2$/TTAB micellar aggregate, the porphyrin and phenyl ring resonances of all micellar systems are of little investigative value, since the resonances are considerably broadened and the signal intensity is low due to the small porphyrin concentrations in the micelles. These signals were, therefore, not further analyzed and their line broadening, which is most likely attributable to the reduced tumbling of the porphyrin inside the micelles, was simply taken as evidence that the porphyrins are embedded in the micelles. This is also supported by the observation that at different pH values the porphyrin and the phenyl ring resonances of all systems are also significantly line-broadened, which allows us to rule out that the pH of the micellar solutions is the major contributor to the line-broadening.

To obtain meaningful information on the factors that modulate the incorporation characteristics of the porphyrins in the micelles, the ^{1}H and ^{13}C chemical shift changes of the TTAB, SDS, and TX-100 surfactant resonances were analyzed. There are ample examples in the literature, which illustrate that both ^{1}H and ^{13}C NMR spectroscopy can be used to probe the location and orientation of molecules in micellar interfaces by means of the chemical shift changes observed for the surfactant resonances.[58−62] For organic anions bound to cationic micellar interfaces, it has been shown that the surfactant resonances shift in a characteristic fashion upon increase in aggregate concentration. The ^{1}H resonances of the headgroup region shift upfield and those further down the alkyl chain shift downfield.[58−62] For porphyrins, such as TPPS$_4$ in CTAB micelles, Kadish et al. have attributed the downfield ^{1}H shifts of the headgroup region, the upfield shift of the terminal methyl group resonances, and the

(57) Ried, S. Master's Thesis, San Francisco State University, San Francisco, CA, 1999.
(58) Bachofer, J. S.; Simonis, U.; Nowicki, T. A. *J. Phys. Chem.* **1991**, *85*, 480−488.
(59) Bachofer, S. J.; Simonis, U. *Langmuir* **1996**, *12* (7), 1744−1754.
(60) (a) Magid, L. J.; Han, Z.; Warr, G. G.; Cassidy, M. A.; Butler, P. D.; Hamilton, W. A. *J. Phys. Chem. B* **1997**, *101*, 7919−7927. (b) Kreke, P. J.; Magid, L.; Gee, J. C. *Langmuir* **1996**, *12*, 699−705. (c) Carver, M.; Smith, T. L.; Gee, J. C.; Delichere, A.; Caponetti, E.; Magid, L. J. *Langmuir* **1996**, *12*, 691−698.
(61) Bunton, C. A.; Nome, F.; Quina, F. H.; Romsted, L. S. *Acc. Chem. Res.* **1991**, *24* (12), 115.
(62) Bunton, C.; Minch, M. J. *J. Phys. Chem.* **1974**, *78* (15), 1490−1498.

Table 3. ^{1}H NMR Chemical Shift Data (δ and $\Delta\delta$, ppm)

(a) 20 mM TTAB Micellar Solutions in the Absence and Presence of Porphyrins (p-COO^-)$_1$TPPH$_2$ **2** and (p-OH)$_1$TPPH$_2$ **3**

	α-CH_2−		-N^+(−CH_3)$_3$		β-CH_2−		γ-CH_2−		(−CH_2−)$_{10}$		ω-CH_3	
	δ	$\Delta\delta$	δ	$\Delta\delta$	δ	$\Delta\delta$	δ	$\Delta\delta$	δ	$\Delta\delta$	δ	$\Delta\delta$
TTAB, neutral	3.347		3.111		1.729		1.323		1.243		0.824	
0.22 mM **2**	3.343	0.004	3.111	0	1.730	−0.001	1.318	0.005	1.227	0.016	0.817	0.007
0.71 mM **3**	3.381	−0.034	3.144	−0.033	1.742	−0.013	1.316	0.007	1.204	0.039	0.804	0.020
TTAB, pH 10	3.456		3.198		1.755		merged		1.256		0.843	
0.30 mM **2**	3.446	0.010	3.210	−0.012	1.747	0.008	merged		1.157	0.099	0.797	0.046
0.16 mM **3**	3.454	0.002	3.196	0.002	1.733	0.022	merged		1.233	0.023	0.839	0.004

(b) 20 mM SDS Micellar Solutions in the Absence and Presence of Porphyrin (p-NH_3^+)$_1$TPPH$_2$ **4** at 298 K

	α-CH_2−		β-CH_2−		(−CH_2−)$_9$		ω-CH_3	
	δ	$\Delta\delta$	δ	$\Delta\delta$	δ	$\Delta\delta$	δ	$\Delta\delta$
SDS, pH 2	4.019		1.673		1.296		0.876	
0.21 mM **4**	4.008	0.011	1.652	0.021	1.265	0.031	0.860	0.016

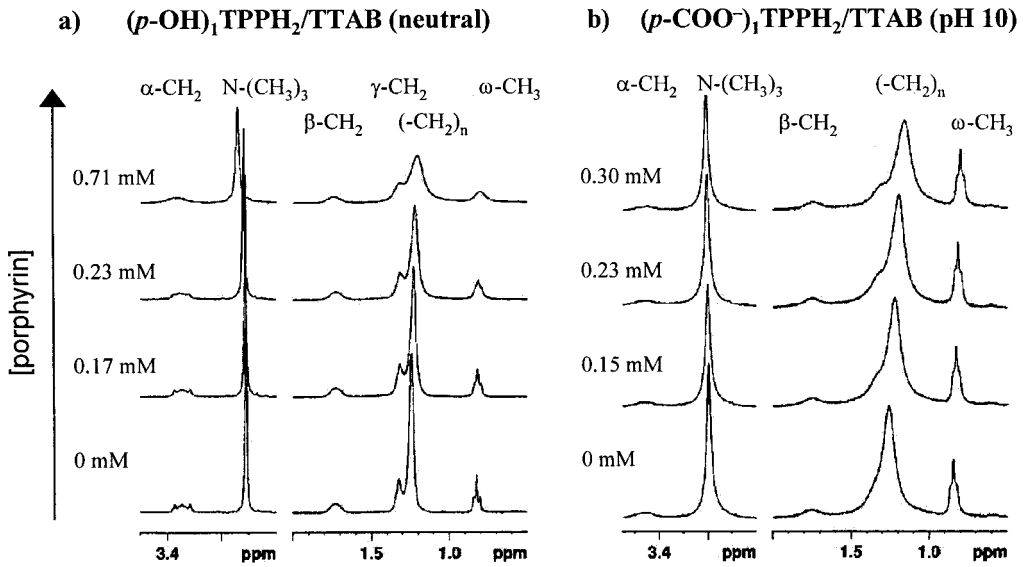

Figure 4. ^{1}H NMR spectra of TTAB micellar solutions in the absence (bottom row) and in the presence of increasing concentrations of (a) (p-OH)$_1$TPPH$_2$ in neutral solution and (b) (p-COO^-)$_1$TPPH$_2$ at pH = 10.

splitting of the methylene peak resonances to porphyrin−micelle interactions.[31,32]

Interactions between (p-COO^-)$_1$TPPH$_2$/(p-OH)$_1$-TPPH$_2$ and Cationic TTAB Micelles. The chemical shifts of the proton resonances of 20 mM TTAB solution in D_2O and in ammonia buffer (pH 10) are listed in Table 3a, together with those of (p-COO^-)$_1$TPPH$_2$- and (p-OH)$_1$-TPPH$_2$-bound TTAB micelles at the highest porphyrin concentrations. The corresponding ^{1}H NMR spectra of TTAB micelles alone (spectrum on the bottom) and of TTAB micelles with incorporated (p-OH)$_1$TPPH$_2$ and (p-COO^-)$_1$TPPH$_2$ are shown in parts a and b of Figure 4, respectively. The chemical shifts of the TTAB headgroup protons (N−(CH_3)$_3$, α-CH_2, β-CH_2) and those of the hydrophobic alkyl chain protons (γ-CH_2, (CH_2)$_{10}$, ω-CH_3) as a function of increasing porphyrin concentration are plotted in Figure 5.

In the presence of (p-OH)$_1$TPPH$_2$, all TTAB resonances are shifted with increasing porphyrin concentration in comparison to TTAB alone. While the resonances of the polar headgroups become deshielded and move downfield, the resonances further down the hydrophobic alkyl chain (γ-CH_2, (CH_2)$_{10}$, ω-CH_3) are shifted upfield as the (p-OH)$_1$TPPH$_2$ concentration increases (Figures 4a and 5a). These shifts are accompanied by significant broadening of all TTAB resonance (Figure 4a). The ^{13}C surfactant signals of the (p-OH)$_1$TPPH$_2$/TTAB micellar aggregates reveal a similar chemical shift pattern (data not shown). These ^{1}H and ^{13}C chemical shift trends imply that (p-OH)$_1$TPPH$_2$ interacts with all groups of the surfactant to a similar extent and suggest that it may be intercalated among the surfactant chains, most likely with the hydroxy substituent extending into the polar headgroup region of the micelle. Such positioning is also consistent with the capability of the hydroxy substituent to form hydrogen bonds to the water molecules in the polar headgroup region of the micelle. Although (p-OH)$_1$TPPH$_2$ seems to localize in more polar domains of the micellar aggregate, it is still residing in an overall hydrophobic environment, which is in agreement with the UV−vis spectroscopic data. Added evidence that (p-OH)$_1$TPPH$_2$ may be intercalated among the surfactant chains is provided by the spin−lattice relaxation times T_1, which serves as additional probe of the porphyrin location within the micellar aggregate.[63] The incorporation of a porphyrin into micelles is expected to lead to changes in the dynamics of the surfactant chains, and most likely to a reduced mobility of the surfactant chains, which is observable in the T_1 relaxation times. When compared to TTAB alone, T_1 of the ω-methyl signal of the (p-OH)$_1$TPPH$_2$/TTAB aggregate is significantly decreased from 1144 ± 2 ms for TTAB alone to 869 ± 22 ms for the 0.71 mM (p-OH)$_1$TPPH$_2$ micellar aggregate. Provided that the condition $\omega_0\tau_c \ll 1$ in the motional

(63) Lindman, B.; Olsson, U. *Ber. Bunsen-Ges. Phys. Chem.* **1996**, *100* (3), 344−363.

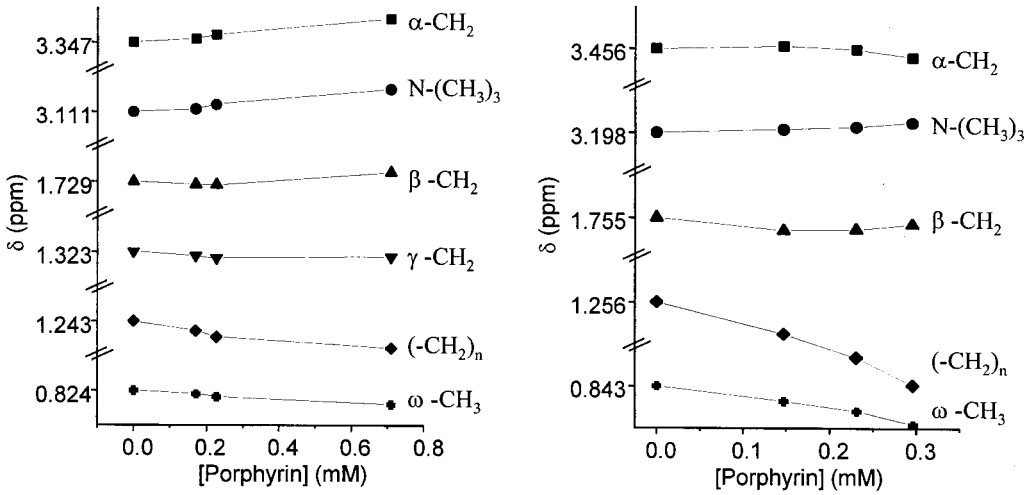

Figure 5. ^{1}H Chemical shift trends of the surfactant resonances of (a) TTAB/(p-OH)$_1$TPPH$_2$ in neutral solution and (b) TTAB/(p-COO$^-$)$_1$TPPH$_2$ at pH = 10 as a function of increasing porphyrin concentration: α-CH$_2$ (■), N−(CH$_3$)$_3$ (●), β-CH$_2$ (▲), γ-CH$_2$ (▼), (−CH$_2$)$_n$ (◆), ω-CH$_3$ (•).

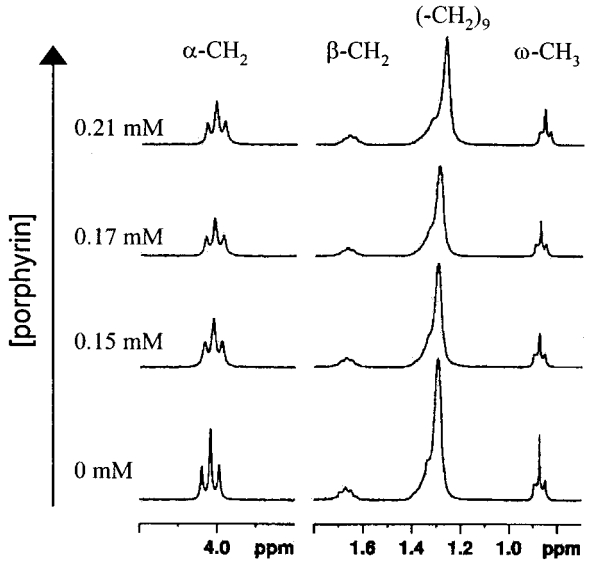

Figure 6. ^{1}H NMR spectra of SDS micellar solutions in the absence (bottom row) and in the presence of increasing concentrations of (p-NH$_3^+$)$_1$TPPH$_2$ at pH = 2.

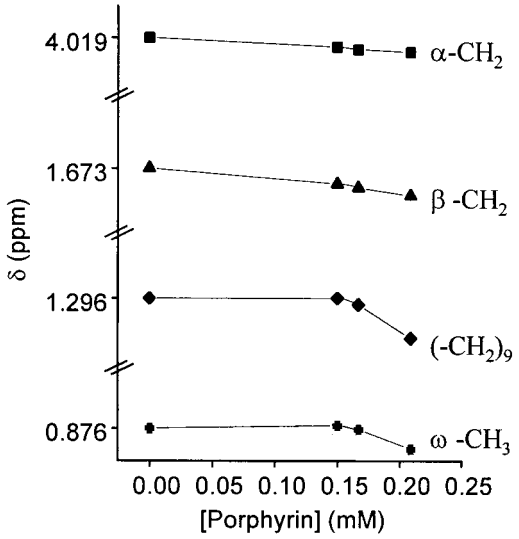

Figure 7. ^{1}H chemical shift trends of the surfactant resonances of SDS/(p-NH$_3^+$)$_1$TPPH$_2$ at pH = 2 as a function of increasing porphyrin concentration: α-CH$_2$ (■), β-CH$_2$ (▲), (−CH$_2$)$_9$ (◆), ω-CH$_3$ (•).

narrowing regime applies for TTAB micellar solutions, the observed decrease in T_1 of the ω-CH$_3$ group implies an increase in its correlation time τ_c and indicates that the motion of the terminal methyl group is restricted, which is most likely due to the interaction with the porphyrin.

Incorporation of (p-COO$^-$)$_1$TPPH$_2$ into TTAB micelles in neutral and basic solution leads to significant upfield shifts for the ^{1}H resonances of the methylene group protons ((CH$_2$)$_{10}$) and those of the terminal methyl group (ω-CH$_3$) of the hydrocarbon chain (Figures 4b and 5b) in comparison to TTAB alone. Furthermore, an additional resonance emerges in the spectral region between 1.3 and 1.4 ppm from the envelope of the methylene peak with increasing (p-COO$^-$)$_1$TPPH$_2$ concentration. However, the proton resonances of the polar headgroup region are little affected by the micellar incorporation of the porphyrin and remain essentially unchanged. The ^{1}H NMR chemical shift trends are also mirrored in the ^{13}C NMR spectra (data not shown). Thus, the chemical shift changes observed suggest that (p-COO$^-$)$_1$TPPH$_2$ interacts preferentially with the inner alkyl chains of the TTAB micelles and infers that this porphyrin is located deeper in the hydrophobic core of the TTAB micelle than (p-OH)$_1$TPPH$_2$. Additional evidence that (p-COO$^-$)$_1$TPPH$_2$ is embedded in the micellar interface and not intercalated among the surfactant chains is provided by the fact that, when compared to (p-OH)$_1$TPPH$_2$, the TTAB resonances are less line-broadened with an increase in porphyrin concentration. This indicates that the surfactant molecules of the (p-COO$^-$)$_1$TPPH$_2$/TTAB aggregate are less restricted in motion, since the porphyrin resides inside the micellar core and is most likely not intercalated among the surfactant chains, which would decrease the surfactant mobility due to the close proximity of guest and host molecules. Although one might expect that the carboxy group would tend to orient itself toward the polar micelle region by, for example, hydrogen bond formation to water at the water−micelle interface, reports by Ricchelli et al.[24−26] agree with our interpretation. Despite the polar COO$^-$ group, protoporphyrin IX is reported to localize in the hydrophobic interior of a bilayer.[25] Thus, porphyrin hydrophobicity seems to be the dominant factor in dictating the location of (p-COO$^-$)$_1$-TPPH$_2$ in the hydrophobic core of the TTAB micellar interface.

Table 4. ^{1}H NMR Chemical Shift Data (δ and $\Delta\delta$, ppm)

(a) ^{1}H NMR Chemical Shift Data of 20 mM TX-100 Micellar Solutions in the Absence and Presence of Porphyrins (p-COO^-)$_1$TPPH$_2$ **2**, (p-OH)$_1$TPPH$_2$ **3**, and (p-NH_3^+)$_1$TPPH$_2$ **4** at 298 K

	3,5-H		2,6-H		-CH_2OH		-CH_2-		-$(CH_3)_2$		-$(CH_3)_3$	
	δ	$\Delta\delta$	δ	$\Delta\delta$	δ	$\Delta\delta$	δ	$\Delta\delta$	δ	$\Delta\delta$	δ	$\Delta\delta$
TX-100, neutral	7.169		6.791		3.993		1.619		1.248		0.670	
0.22 mM **2**	7.111	0.058	6.735	0.056	3.938	0.055	1.570	0.049	1.196	0.052	0.627	0.043
1.36 mM **3**	7.116	0.053	6.749	0.043	3.956	0.037	1.570	0.049	1.198	0.050	0.627	0.043
0.35 mM **4**	7.122	0.047	6.748	0.044	3.950	0.043	1.579	0.040	1.205	0.043	0.632	0.038
TX-100, pH 10	7.161		6.787		3.992		1.612		1.240		0.663	
0.29 mM **2**	7.044	0.117	6.678	0.110	3.884	0.108	1.514	0.098	1.139	0.101	0.579	0.084
1.09 mM **3**	7.064	0.098	6.693	0.095	3.887	0.105	1.528	0.084	1.154	0.086	0.592	0.071
TX-100, pH 2	7.166		6.790		3.993		1.618		1.246		0.669	
0.57 mM **4**	7.079	0.087	6.706	0.083	3.914	0.079	1.545	0.073	1.173	0.073	0.604	0.065

(b) ^{1}H NMR Chemical Shift Data of the Polar Headgroup ($-O-CH_2-CH_2)_n$ Resonances in the Spectral Region between 3.5 and 3.8 ppm of 20 mM TX-100 Micellar Solutions in the Absence and Presence of Porphyrins (p-COO^-)$_1$TPPH$_2$ **2**, (p-OH)$_1$TPPH$_2$ **3**, and (p-NH_3^+)$_1$TPPH$_2$ **4** at 298 K[a]

	1	2	3	4	5	6	7	8	9	10	11
TX-100, neutral	3.709					3.660	3.651	3.640	3.627	3.609	3.596
0.22 mM **2**	3.707			3.669	3.662	3.653	3.643	3.631	3.616	3.598	3.579
	(0.002)					(0.007)	(0.008)	(0.009)	(0.011)	(0.011)	(0.017)
1.36 mM **3**	3.709		3.679	3.674	3.667	3.659	3.649	3.638	3.623	3.606	3.589
	(0)					(0.001)	(0.002)	(0.002)	(0.004)	(0.003)	(0.007)
0.35 mM **4**	3.702	3.677	3.672	3.666	3.659	3.650	3.640	3.628	3.613	3.596	3.577
	(0.007)					(0.010)	(0.011)	(0.012)	(0.014)	(0.013)	(0.019)
TX-100, pH 10	3.717		3.684	3.678	3.671	3.663	3.653	3.640	3.623	3.610	3.596
0.29 mM **2**	3.721	3.685	3.678	3.671	3.662	3.652	3.640	3.624	3.604	3.587	3.568
	(−0.004)		(0.006)	(0.007)	(0.009)	(0.011)	(0.013)	(0.016)	(0.019)	(0.023)	(0.028)
1.09 mM **3**	3.721	3.684	3.677	3.670	3.661	3.651	3.638	3.622	3.601	3.583	3.562
	(−0.004)		(0.007)	(0.008)	(0.010)	(0.012)	(0.015)	(0.018)	(0.022)	(0.027)	(0.034)
TX-100, pH 2	3.709	3.685	3.681	3.675	3.668	3.661	3.652	3.641	3.627	3.610	3.595
0.57 mM **4**	3.718	3.690	3.681	3.675	3.668	3.659	3.649	3.637	3.622	3.604	3.584
	(−0.009)	(−0.005)	(0)	(0)	(0)	(0.002)	(0.003)	(0.004)	(0.005)	(0.006)	(0.011)

[a] The resonances are numbered 1−11 according to their appearances in the NMR spectra from downfield to upfield positions.

Interactions between (p-NH_3^+)$_1$TPPH$_2$ and Anionic SDS Micelles. For the (p-NH_3^+)$_1$TPPH$_2$/SDS aggregate similar conclusions to those derived from UV−vis spectroscopy can be drawn from the analysis of the observed ^{1}H NMR chemical shift changes, which reveal that **4** incorporates into the hydrophobic interior of SDS micelles under acidic conditions. The ^{1}H NMR chemical shifts of SDS alone (bottom row) and in the presence of increasing amounts of (p-NH_3^+)$_1$TPPH$_2$ at pH 2 are shown in Figure 6. The chemical shift changes of the SDS protons as a function of porphyrin concentration are given in Figure 7 and are summarized for the highest porphyrin concentration in Table 3b.

The resonance of the methylene groups of the SDS hydrocarbon chain exhibits the largest upfield shift with increasing (p-NH_3^+)$_1$TPPH$_2$ concentration, whereas the signals of the polar headgroup (α,β-CH_2) are insignificantly upfield-shifted (Figures 6 and 7). Upon incorporation into the micellar environment, all resonances display an increased line broadening (Figure 6). The chemical shift changes and the line broadening again are indicative that the porphyrin interacts with SDS micelles. This interaction is similar to that of (p-COO^-)$_1$TPPH$_2$ with TTAB micelles and suggests that (p-NH_3^+)$_1$TPPH$_2$ localizes in the hydrophobic core of the SDS micelles rather than being intercalated among the surfactant chains and drawn to the micellar surface by hydrogen bond formation or electrostatic interactions, which would result in larger shifts for the polar headgroup signals. Again, porphyrin hydrophobicity seems to dictate the location of this porphyrin in SDS micelles.

Interactions between Porphyrins 2−4 and Nonionic TX-100 Micelles. Micelles formed by nonionic TX-100 surfactants are less selective in solubilizing porphyrins when compared to TTAB and SDS micelles. With the exception of **1**, all other porphyrins dissolve in TX-100 micelles independent of the charge and polarity of the porphyrin substituent and the pH of the solution. Table 4 lists the chemical shifts of all TX-100 protons in neutral, basic (pH 10), and acidic (pH 2) solution in the absence and presence of various amounts of (p-OH)$_1$TPPH$_2$, (p-COOH/COO^-)$_1$TPPH$_2$, and (p-NH_2/NH_3^+)$_1$TPPH$_2$. A representative ^{1}H NMR spectrum of (p-COO^-)$_1$TPPH$_2$ in TX-100 at pH = 10 is shown in Figure 8 and exemplifies the chemical shift trends observed for all other TX-100 micellar aggregates. Figure 8 depicts the ^{1}H chemical shift changes of all surfactant resonances at pH = 10 in the absence (bottom row) and presence of increasing (p-COO^-)$_1$TPPH$_2$ concentrations. The polyoxyethylene group that comprises the polar head group region of TX-100 micelles gives rise to a broad composite peak in the spectral region of 3.5−3.75 ppm, which is split into a maximum of 11 not completely resolved signals. Their chemical shifts are listed in Table 4b. The signals of the phenyl ring protons are observed in the spectral region of 6.8−7.4 ppm, those of the alkyl chain protons resonate between 0.6 and 1.7 ppm, and the signal of the methylene protons attached to the ether or alcohol function give rise to the broad resonances at 3.75 and 3.9 ppm, respectively. The chemical shifts of the TX-100 protons as a function of porphyrin concentration are depicted in Figure 9. The plots of the other TX-100 micellar systems reveal similar trends and are therefore not shown.

Porphyrin incorporation into TX-100 micelles leads to an increased spread of the polyoxyethylene resonances and an upfield bias for all other resonances. The largest shifts are observed for the protons furthest down the polyoxyethylene group. The signals of the alkyl group and the phenyl ring protons shift to a similar extent. These shifts are caused by the porphyrin incorporation into the

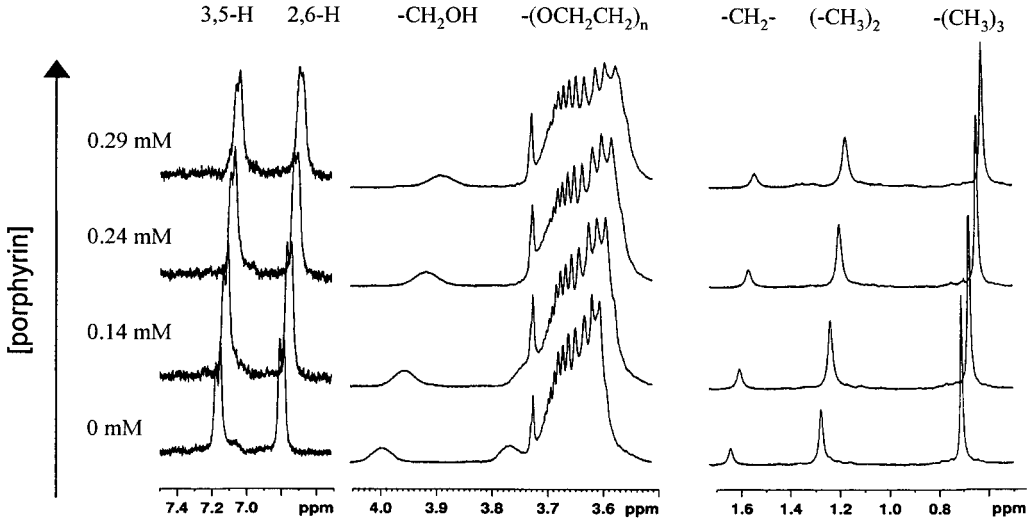

Figure 8. Representative ^{1}H NMR spectra of TX-100 micellar solutions in the absence (bottom row) and in the presence of increasing concentrations of (p-COO^-)$_1$TPPH$_2$ at pH = 10.

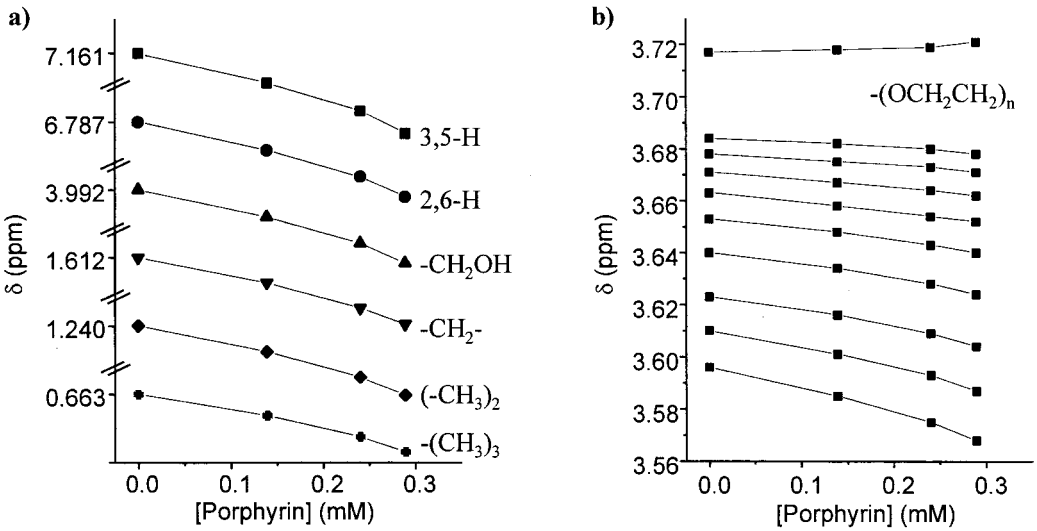

Figure 9. ^{1}H chemical shift trends of the surfactant resonances of TX-100/(p-COO^-)$_1$TPPH$_2$ at pH = 10 as a function of increasing porphyrin concentration: (a) resonances of 3,5-H (■), 2,6-H (●), $-CH_2-OH$ (▲), $-CH_2$ (▼), $(-CH_3)_2$ (◆), and $(-CH_3)_3$ (•); (b) resonances of the polar headgroup protons $(-O-CH_2-CH_2)_n$ between 3.5 and 3.8 ppm.

micelle and suggest that all porphyrins interact with both the polar headgroup and the hydrophobic core of TX-100 micelles and that the porphyrins are most likely intercalated among the TX-100 surfactant chains.

Conclusions

In regard to the incorporation characteristics of porphyrins **2**−**4** in TTAB, SDS, and TX-100 micelles, the following general conclusions can be drawn from the UV−visible and the NMR spectroscopy data discussed above: (i) The nature of the porphyrin substituent and the surfactant headgroup determine whether a porphyrin will diffuse into a micellar interface. (ii) At least one polar or charge-bearing substituent in para-position of one of the porphyrin phenyl rings is required to solubilize relatively hydrophobic porphyrins in aqueous micellar solutions. (iii) Polar or charged porphyrins incorporate into nonionic micelles independent of the charge and polarity of the substituent. (iv) Electrostatic interactions between the micelle and the porphyrin seem to play important roles in incorporating porphyrins into cationic and anionic micelles. (v) The presence of an OH group significantly increases the tendency of a porphyrin to dissolve in cationic or nonionic micelles. This result emphasizes the importance of a hydroxy group in solubilizing porphyrins at micellar interfaces and suggests that an OH-substituent placed at the porphyrin periphery may be essential for synthesizing clinically useful porphyrin drugs. Furthermore the data presented in this paper establish that porphyrins, which diffuse into micellar solutions, are monodispersed in given micelles and that the magnitudes of the chemical shift changes observed in the NMR spectra for the surfactant resonances are indicative of the location of the porphyrin within a given micelle. In regard to micellar location and orientation, the following can be concluded: (i) Porphyrins with charged substituents, such as COO^- or NH_3^+, are more deeply embedded in the hydrophobic core of TTAB or SDS micelles, respectively, despite the substituent charge. This is evidenced by the significantly larger chemical shift changes observed for the surfactant methylene resonances closer to the tail and those of the ω-CH_3 group. The hydrophobicity of the porphyrin seems to be the major contributor to this orientation. As is indicated by the comparable chemical shift changes of *all* surfactant resonances, in nonionic micelles these porphyrins seem to localize in more polar

domains of the micelles and to intercalate among the surfactant chains. (ii) The OH−phenyl-substituted porphyrin most likely intercalates among the surfactant chains of TTAB and TX-100 to adopt an orientation in which the hydroxy group is oriented toward the micelle−water interphase. In this case, the hydrogen bond formation of the OH group to the water at the water−micelle interface may be a dominant factor in determining such an orientation.

Acknowledgment. This investigation is in part described in the M.S. Thesis of S. Ried at San Francisco State University. It was supported by a "Research Infrastructure in Minority Institutions" award from the National Center for Research Resources with funding from the Office of Research on Minority Health, National Institutes of Health #5 P20 RR11805, by awards from NSF (Grant CHE-9816356, U.S.), the Camille and Henry Dreyfus Foundation (U.S.), and Research Corporation (U.S.). Support from the Department of Chemistry & Biochemistry and the College of Science & Engineering at San Francisco State University is also greatly acknowledged. The Department of Chemistry & Biochemistry at San Francisco State University acknowledges grants from the NIH (RR 02684) and NSF (DMB-8516065 and DUE-9451624) for the purchase of the NMR spectrometers.

LA990903+